Available online at www.elixirpublishers.com (Elixir International Journal)

Applied Chemistry

Elixir Appl. Chem. 83 (2015) 33075-33082

ISSN: 2229-712X

Density Functional Study and the Vibrational Spectra of 4-Chloro-3, 5-Xylenol

M.K.Subramanian* and S.Revathi

Post Graduate and Research Department of Physics, Thiruvalluvar Government Arts College, Rasipuram, India.

ARTICLE INFO

Article history:

Received: 25 April 2015;

Received in revised form: 2 June 2015;

Accepted: 9 June 2015;

Keywords

Density Functional Theory,
HOMO,
LUMO,
First-order Hyperpolarizability,
Electronic Excitation Energy.

ABSTRACT

The Fourier transform Raman and Fourier transform infrared spectra of 4-chloro-3,5-xylenol (4C35X) have been recorded by using DFT calculations. The theoretical computational density functional theory (DFT/B3LYP) was performed at 6-311+G** levels to derive equilibrium geometry, vibrational wavenumbers, infrared intensities and Raman scattering activities. The complete vibrational assignment was performed on the basis of the potential energy distribution (PED), calculated with scaled quantum mechanics (SQM) method. The Mulliken atomic charges and Dipole moment have been calculated. The first-order hyperpolarizability has been computed using quantum chemical calculations. Electronic excitation energies, oscillator strength and nature of the respective excited states were calculated by the closed-shell singlet calculation method for the molecule.

© 2015 Elixir All rights reserved.

Introduction

4-chloro-3,5-xylenol is a broad spectrum antimicrobial chemical compound used to control bacteria, algae, fungi and virus. It is used in hospitals and households for disinfection and sanitation. It is also commonly used in antibacterial soaps, wound-cleansing applications and household antiseptics such as Dettol liquid, cream and ointments. Studies have shown an anti-microbial activity which is enhanced by additives. Its antibacterial action is due to disruption of cell membrane potentials [1]. 4-chloro-3,5-xylenol is not significantly toxic to humans and other mammals, is practically non-toxic to birds, moderately toxic to freshwater invertebrates and highly toxic to fish. It is a mild skin irritant and may trigger allergic reactions in some individuals. It has been used in other fields such as glue, painting, textile, pulp etc.

In the present study the FT-IR, FT-Raman and theoretical calculations of the wavenumbers of the 4-chloro-3,5-xylenol (4C35X) are reported. Further, density functional theory (DFT) combined with quantum chemical calculations to determine the first-order hyperpolarizability. The calculated HOMO and LUMO energies shows that charge transfer occur within the molecule. Electronic excitation energies, oscillator strength and nature of the respective excited states were calculated by the closed-shell singlet calculation method were also calculated for the molecule.

Experimental Details

The fine sample of 4C35X were obtained from Lancaster Chemical Company, UK, and used as such for the spectral measurements. The room temperature Fourier transform infrared spectra of the title compounds were measured in the region 4000–400 cm^{-1} at a resolution of ±1 cm^{-1} using BRUKER IFS 66V vacuum Fourier transform spectrometer, equipped with an MCT detector, a KBr beam splitter and globar source. The FT-Raman spectra were recorded on the same instrument with FRA 106 Raman accessories in the region 4000–100 cm^{-1}. Nd:YAG laser op-erating at 200mW power with 1064 nm excitation was used as source.

Computational Details

The molecular geometry optimization vibrational frequency calculations were carried out for 4C35X with GAUSSIAN 09W software package [2] using B3LYP functional method combined with standard 6-311+G** basis set [3,4] was applied to represent the molecular orbital. The IR and Raman wave numbers and intensities were computed at the same level of theory using the harmonic approximation and the analytical derivatives procedure incorporated in the GAUSSIAN program. The vibrational modes were assigned by means of visual inspection using the GAUSSVIEW program [5]. The symmetry of the molecule was also helpful in making vibrational assignments. The symmetry of the vibrational modes were determined by using standard procedure of decomposition the traces of the symmetry operations in to the irreducible representations. The Raman activities (Si) calculated by the GAUSSIAN 09W program were converted to relative Raman intensities (Ii) using the following relationship derived from the basic theory of Raman scattering,

$$I_i = \frac{f(v_o - v_i)^4 S_i}{v_i[1-\exp(-hcv_i / KT)} \text{----------(1)}$$

Where υ_0 is the exciting frequency (in cm^{-1}), υ_i is the vibrational wavenumber of the ith normal mode; h, c and k are fundamental constants, and f is a suitably chosen common normalization factor for all peak intensities.

Results and discussion

Geometry optimization

The molecular structure of 4C35X belongs to C_s point group symmetry and shown in Fig 1. The 51 normal modes of vibrations are distributed among the symmetry species as Γ_{3N-6}=35 A′(in plane)+16 A″ (out of plane). All vibrations are active in both the Raman scattering and infrared absorption. The A′ modes be polarized bands in the Raman spectrum. The global minimum energy obtained by the DFT structure optimization for the title compound is presented in Table 1. The bond length, bond angle and dihedral angle determined at the DFT level of theory for the 4C35X compound are listed in Table 2.

Tele:
E-mail addresses: profdrmks@gmail.com

© 2015 Elixir All rights reserved

Vibrational spectra

Detailed description of vibrational mode can be given by means of normal coordinate analysis (NCA). For this purpose, the set of 65 standard internal coordinates containing 14 redundancies are defined as given in Table 3. From these a non-redundant set of local symmetry coordinates were constructed by suitable linear combination of internal coordinates following the recommendations of Fogarasi et al. [6] are summarized in Table 4. The theoretically calculated DFT force fields were transformed to this later set of vibrational coordinates and used in all subsequent calculations.

For visual comparison, the observed and stimulated FT-IR and FT-Raman spectra of the title compound are presented in Fig 2 and Fig 3, respectively. Comparison between calculated and observed vibrational spectra helps us to understand the observed spectral features. The results of vibrational analysis, viz., calculated vibrational frequencies, IR intensities and assignment of the fundamentals for the title compound are collected in Table 5.

Root mean square (RMS) values of frequencies were obtained in the study using the following expression,

$$\mathrm{RMS} = \sqrt{\frac{1}{n-1}\sum_{i}^{n}\left(\upsilon_i^{calc} - \upsilon_i^{exp}\right)^2}$$

The RMS error of the observed and calculated frequencies (unscaled / B3LYP/6-311+G**) of 4C35X was found to be 103 cm^{-1}. In order to reduce the overall deviation between the unscaled and observed fundamental frequencies, scale factors were applied in the normal coordinate analysis and the subsequent least square fit refinement algorithm resulted into a very close agreement between the observed fundamentals and the scaled frequencies. Refinement of the scaling factors applied in this study achieved a weighted mean deviation of 7.42 cm^{-1} between the experimental and scaled frequencies of the title compound.

C−C vibrations

The ring carbon-carbon stretching vibrations occur in the region 1680-1430 cm^{-1}. In the present work, the frequencies observed in the FT-IR spectrum at 1657, 1654, 1653, 1476, 1467 and 1449 cm^{-1} have been assigned to C−C stretching vibrations. The corresponding vibrations appear in the FT-Raman spectrum at 1670, 1669, 1667, 1516, 1515, 1511, 1385 and 1381 cm^{-1}. The in plane deformation vibration is at higher frequencies than the out-of-plane vibrations [7].

C-O vibrations

In general the characteristic C-O stretching vibrations are found in the region 1400-1000 cm^{-1} depending on the ring size. The C-O frequencies increase with ring strain. The 4C35X shows bands at 1385, 1384, 1381, 1380, 1217, 1213 and 1209 cm^{-1} respectively. The increase in frequency has established strain on the ring and the intensity of the carbonial band is essentially the same in all compounds [8,9]. The stretching vibrations of single bonded carbon and oxygen atoms have been noticed at 1069, 1066 and 1065 cm^{-1}.

O–H group vibrations

The O-H stretching vibrations are normally observed at about 3800-3400 cm^{-1}. The O-H in-plane bending vibration is observed in the region 1440–1100 cm^{-1} [10]. The FTIR band appeared at 3759, 3757 and 3755 cm^{-1} was assigned to O-H stretching modes of vibrations. The in-plane and out-of-plane bending vibrations of hydroxy groups have been identified at 1289, 1287, 1282 and 1240, 1236, 1233 cm^{-1} for 4C35X, respectively.

C-H vibrations

The aromatic structure shows the presence of C–H stretching vibrations in the region 3300-3100 cm^{-1} which is the characteristic region for the ready identification of such C–H stretching vibrations [11,12]. Accordingly, in the present study, the C-H vibrations are observed at 3215, 3216 and 3213 cm^{-1} in the FT-Raman spectrum and at 3172, 3169 and 3168 cm^{-1} in the FT-IR for 4C35X. The C-H in-plane and out-of-plane bending vibrations have also been identified and presented in Table 5.

Ring vibrations

Several ring modes are affected by the substitution to the aromatic ring of 4C35X. In the present study, the bands ascribed at 1385, 1384, 1381, 1380, 1075, 1073, 1071, 1069, 1066, 1065, 849, 848, 846 and 841 cm^{-1} for 4C35X have been designated to ring in-plane and out-of-plane bending modes, respectively, by careful consideration of their quantitative descriptions. A small change in frequency observed for these modes are due to the changes in force constant/reduced mass ratio.

C–Cl vibration

The C-Cl stretching gives generally strong bands in the 800–505 cm^{-1} region [13]. The sharp FT-IR and FT-Raman bands at 646, 642, 640 cm^{-1} and 570, 569, 566 cm^{-1} respectively observed in the spectrum of the title compound are assigned to C-Cl stretching vibration.

Methyl group vibrations

The 4C35X compound, under consideration possesses only one CH_3 group in third position of the ring, respectively. For the assignments of CH_3 group frequencies, one can expect that nine fundamentals can be associated to each CH_3 group, namely the symmetrical (CH_3 ips) and asymmetrical (CH_3 ops), in plane stretching modes (i.e. in-plane hydrogen stretching mode); the symmetrical (CH_3 ss), and asymmetrical (CH_3 ips), deformation modes; the in-plane rocking (CH_3 ipr) out-of-plane rocking (CH_3 opr) and twisting (t CH_3) bending modes. In addition to that, the asymmetric stretching (CH_3 ops) and asymmetric deformation (CH_3 opb) modes of the CH_3 group are expected to be depolarised for A'' symmetry species. The FT-IR and Raman bands at 3155, 3152, 3141, 3140, 3137, 3122, 3120, 3118, 3106 and 3063 cm^{-1} represent symmetric and asymmetric CH_3 stretching vibrations of the methyl group in 4C35X. The fundamental vibrations arising from symmetric, asymmetric in-plane and out-of-plane deformations, rocking and twisting modes of CH_3 group 4C35X are observed in their respective characteristic regions and they are listed in Table 5 respectively.

Mulliken charges and Dipole moment

Dipole moment reflects the molecular charge distribution and is given as a vector in three dimensions. Therefore, it can be used as descriptor to depict the charge movement across the molecule. Direction of the dipole moment vector in a molecule depends on the centers of positive and negative charges. Dipole moments are strictly determined for neutral molecules. For charged systems, its value depends on the choice of origin and molecular orientation.

Mulliken atomic charge calculation has an important role in the application of quantum chemical calculations to molecular system because of atomic charges affect dipole moment, molecular polarizability, electronic structure and more a lot of properties of molecular systems. The charge distributions calculated by the Mulliken [14] and NBO methods for the equilibrium geometry of 4C35X are listed in Table 6.

First-order hyperpolarizability calculations

In the presence of an applied electric field, first-order hyperpolarizability is a third rank tensor that can be described by a 3×3×3 matrix. The components of the 3D matrix can be

reduced to 10 components because of the Kleinman symmetry [15]. The matrix can be given in the lower tetrahedral format. It is obvious that the lower part of the 3×3×3 matrix is a tetrahedral. The calculation of NLO properties with high accuracy is challenging and requires consideration of many different issues. Computational techniques are becoming valuable in designing, modeling and screening novel NLO materials. The calculated first-order hyperpolarizability (β_{total}) of 4C35X is 34.726×10^{-30} esu, which is greater than that of urea (0.1947×10^{-30} esu). The calculated values of dipole moment and hyperpolarizability values are tabulated in Table 7. The β_{yzz} direction shows biggest value of hyperpolarizability which insists that the delocalization of electron cloud is more on that direction than other directions.

Electronic excitation energies, oscillator strength and nature of the respective excited states were calculated by the closed-shell singlet calculation method and are summarized in Table 8. Fig 4 shows the highest occupied molecule orbital (HOMO) and lowest unoccupied molecule orbital (LUMO) of 4C35X. Orbital involved in the electronic transition for (a) HOMO−0 (b) LUMO+0 (c) HOMO-1 (d) LUMO+1 (e) LUMO+2 is represented in Fig 5. The NLO responses can be understood by examining the energetic of frontier molecular orbitals. There is an inverse relationship between hyperpolarizability and HOMO–LUMO.

HOMO energy = -0.003 a.u
LUMO energy = 0.005 a.u
HOMO–LUMO energy gap = 0.008 a.u

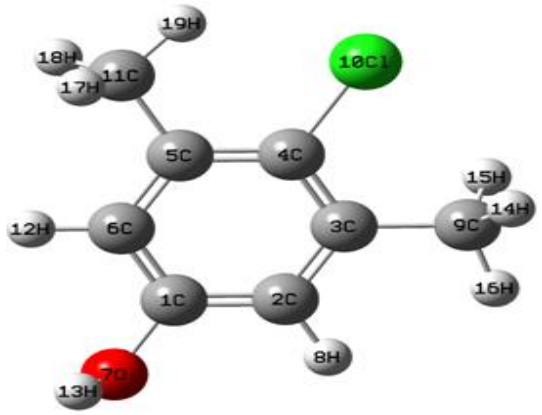

Fig 1. The optimized molecular structure of 4C35X

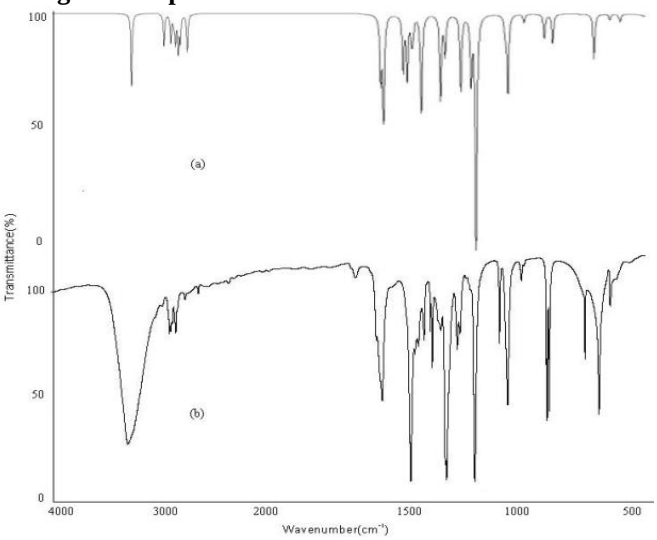

Fig 2. FT-IR spectra of 4C35X
(a)Calculated (b) Observed with B3LYP/6-311+G**

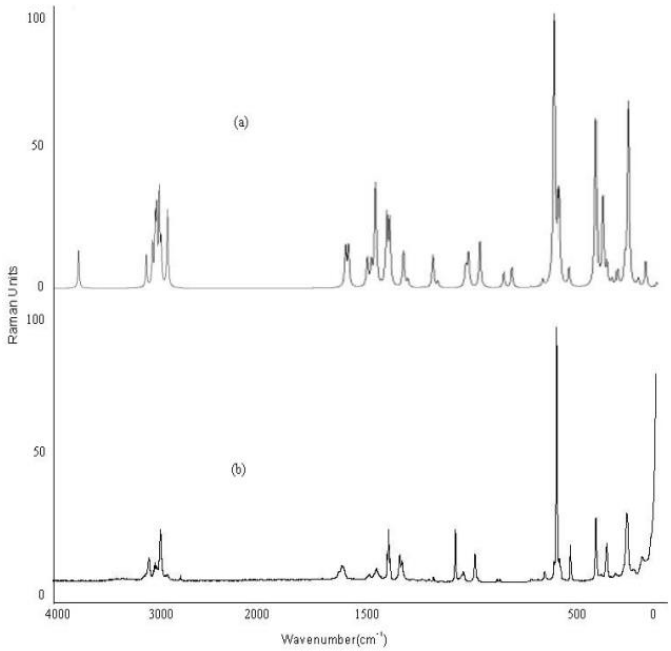

Fig 3. FT-Raman spectra of 4C35X
(a) Calculated (b) Observed with B3LYP/6-311+G**

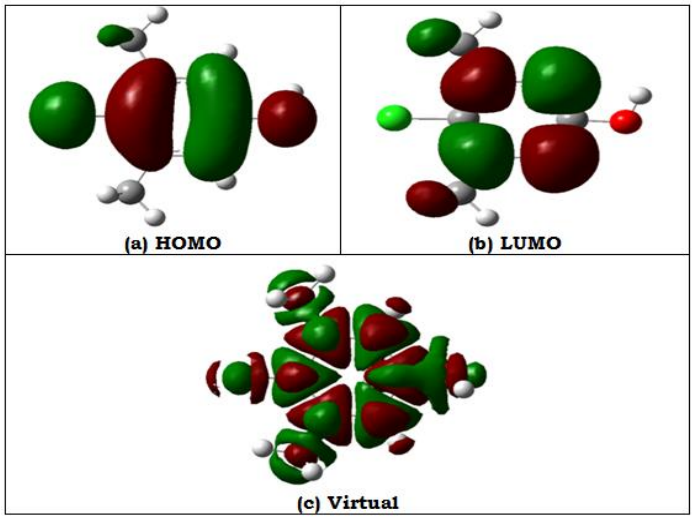

Fig 4. Representation of the orbital involved in the electronic transition for (a) HOMO (b) LUMO (c) Virtual

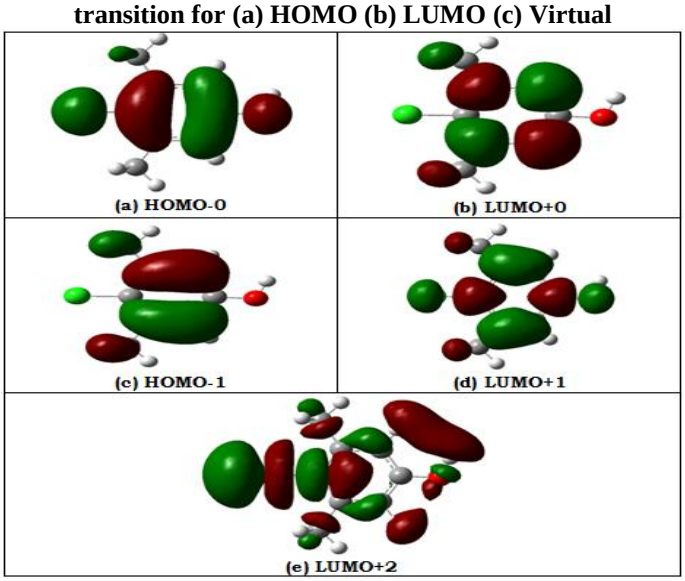

Fig 5. Representation of the orbital involved in the electronic transition for (a) HOMO−0 (b) LUMO+0 (c) HOMO-1 (d) LUMO+1 (e) LUMO+2

Table 1. Total energies of 4C35X, calculated at DFT B3LYP/6-31G* and B3LYP/6-311+G level**

Method	Energies (Hartrees)
6-31G*	-845.57925312
6-311+G**	-845.69712145

Table 2. Optimized geometrical parameters of 4C35X obtained by B3LYP/6–311+G density functional calculations**

Bond length	Value(Å)	Bond angle	Value(Å)	Dihedral angle	Value(Å)
C2-C1	1.38599	C3-C2-C1	120.00023	C4-C3-C2-C1	0.00000
C3-C2	1.38600	C4-C3-C2	120.00023	C5-C4-C3-C2	0.00000
C4-C3	1.38599	C5-C4-C3	119.99953	C6-C1-C2-C3	0.00000
C5-C4	1.38599	C6-C1-C2	119.99953	O7-C1-C2-C3	-179.42757
C6-C1	1.38599	O7-C1-C2	119.99899	H8-C2-C1-C6	-179.42216
O7-C1	1.41005	H8-C2-C1	119.99900	H9-C3-C2-C1	-179.42435
H8-C2	1.12206	H9-C3-C2	119.99513	Cl10-C4-C3-C2	-179.42484
H9-C3	1.54002	Cl10-C4-C3	119.99898	C11-C5-C4-C3	-179.42429
Cl10-C4	1.75996	C11-C5-C4	120.00026	H12-C6-C1-C2	179.42213
C11-C5	1.53994	H12-C6-C1	119.99645	H13-O7-C1-C2	120.00084
H12-C6	1.12197	H13-O7-C1	109.49800	H14-C9-C3-C2	-120.00491
H13-O7	0.99198	H14-C9-C3	109.49663	H15-C9-C3-C2	119.93397
H14-C9	1.12203	H15-C9-C3	109.49928	H16-C9-C3-C2	0.06656
H15-C9	1.12197	H16-C9-C3	109.50731	H17-C11-C5-C4	-119.99898
H16-C9	1.12193	H17-C11-C5	109.50278	H18-C11-C5-C4	119.92899
H17-C11	1.12201	H18-C11-C5	109.50850	H19-C11-C5-C4	0.06648
H18-C11	1.12198	H19-C11-C5	109.49962		
H19-C11	1.12203				

*for numbering of atom refer Fig 1

Table 3. Definition of internal coordinates of 4C35X

No(i)	symbol	Type	Definition
Stretching 1-6	r_i	C-C	C1-C2,C2-C3,C3-C4,C4-C5,C5-C6,C6-C1
7-8	S_i	C-H	C2-H8,C6-H12
9	p_i	C-Cl	C4-Cl10
10	δ_i	C-O	C1-O7
11	$\square_i$	O-H	O7-H13
12-13	P_i	C-C(m)	C3-C9,C5-C11
14-16	n_i	C-H(m)	C9-H14,C9-H15,C9-H16
17-19	N_i	C-H(m)	C11-H17,C11-H18,C11-H19
Bending 20-25	α_i	C-C-C	C1-C2-C3,C2-C3-C4,C3-C4-C5, C4-C5-C6,C5-C6-C1,C6-C1-C2
26-29	θ_i	C-C-H	C3-C2-H8, C1-C2-H8,C1-C6-H12, C5-C6-H12
30-31	β_i	C-C-Cl	C3-C4-Cl10, C5-C4-Cl10
32-33	X_i	C-C-O	C2-C1-O7, C6-C1-O7
34	w_i	C-O-H	C1-O7-H13
35-38	Φ_i	C-C-C	C4-C3-C9, C2-C3-C9,C4-C5-C1, C6-C5-C11
39-41	μ_i	H-C-H	H14-C9-H15,H15-C9-H16, H16-C9-H14
42-44	ν_i	C-C-H	C3-C9-H14,C3-C9-H15, C3-C9-H16
45-47	ε_i	H-C-H	H17-C11-H18, H18-C11-H19, H19-C11-H17
48-50	ι_i	C-C-H	C5-C11-H17,C5-C11-H18,C5-C11-H19
Out-of-plane 51-52	ω_i	C-H	H8-C2-C1-C3, H12-C6-C1-C5
53	ξ_i	C-Cl	Cl10-C4-C3-C5
54	$\&_i$	C-O	O7-C1-C2-C6
55-56	Ω_i	C-C	C9-C3-C4-C2, C11-C5-C4-C6
Torsion 57-62	τ_i	C-C	C1-C2-C3-C4,C2-C3-C4-C5,C3-C4-C5-C6,C4-C5-C6-C1, C5-C6-C1-C2,C6-C1-C2,C3
63	τ_i	O-H	H13-O7-C1-C2(C6)
64	τ_i	C-H	C2-C3-C9-(H14,H15,H16)
65	τ_i	C-H	C6-C5-C11-(H17,H18,H19)

*for numbering of atom refer Fig 1

Table 4. Definition of local symmetry coordinates and the value corresponding scale factors used to correct the force fields for 4C35X

No.(i)	Symbol[a]	Definition[b]	Scale factors used in calculation
1-6	C-C	r1,r2,r3,r4,r5,r6	0.914
7-8	C-H	S7,S8	0.914
9	C-Cl	p9	0.992
10	C-O	δ10	0.992
11	O-H	□11	0.992
12-13	C-Cm	P12,P13	0.992
14	mss1	(n14+n15+n16)/ √3	0.995
15	mips1	(2n15-n14-n16)/ √6	0.992
16	mops1	(n15-n16)/ √2	0.919
17	mss2	(N17+N18+N19)/ √3	0.919
18	mips2	(2N18-N17-N19)/ √6	0.919
19	mops2	(N18-N19)/ √2	0.919
20	C-C-C	(α20-α21+α22-α23+α24-α25)/ √6	0.992
21	C-C-C	(2α20-α21-α22+2α23-α24-α25)/ √12	0.992
22	C-C-C	(α21-α22+α24-α25)/2	0.992
23-24	C-C-H	(θ26-θ27)/√2,(θ28-θ29)/√2	0.916
25	C-C-Cl	(β30-β31)/√2	0.923
26	C-C-O	(X32-X33)/√2	0.923
27	C-O-H	w34	0.922
28-29	C-C-C	(Φ35- Φ36)/√2, (Φ37- Φ38)/√2	0.923
30	msb1	(μ39+μ40+μ41-ν42-ν43-ν44)/ √6	0.990
31	mipb1	(2μ41-μ39-μ40)/ √6	0.990
32	mopb1	(μ39-μ41)/ √2	0.990
33	mipr1	(2ν43-ν42-ν44)/ √6	0.990
34	mopr1	(ν42-ν44)/ √2	0.990
35	msb2	(ε45+ε46+ε47-ι48-ι49-ι50)/ √6	0.990
36	mipb2	(2ε47-ε45-ε46)/ √6	0.990
37	mopb2	(ε45-ε47)/ √2	0.990
38	mipr2	(2ι49-ι48-ι50)/ √6	0.990
39	mopr2	(ι48-ι50)/ √2	0.990
40-41	C-H	ω51, ω52	0.994
42	C-Cl	ξ53	0.962
43	C-O	&54	0.962
44-45	C-C	Ω55, Ω56	0.962
46	tring	(τ57-τ58+τ59-τ60+τ61-τ62)/√6	0.994
47	tring	(τ57-τ59+τ60-τ62)/2	0.994
48	tring	(-τ57+2τ58-τ59-τ60+2τ61-τ62)/√12	0.994
49	C-H	τ63/2	0.979
50	O-H	τ64/3	0.979
51	C-H	τ65/3	0.979

These symbols are used for description of the normal modes by TED in Table 5.
The internal coordinates used here are defined in Table 3.

Table 5. Detailed assignments of fundamental vibrations of 4C35X by normal mode analysis based on SQM force field calculation

S. No.	Symmetry species C_s	Observed frequency (cm^{-1})		Calculated frequency (cm^{-1}) with B3LYP/6-311+G** force field				TED (%) among type of internal coordinates[c]
		Infrared	Raman	Unscaled	Scaled	IR[a] A_i	Raman[b] I_i	
1	A'	3759		3757	3755	44.070	125.311	OH(100)
2	A'		3215	3216	3213	19.440	62.544	CH(99)
3	A'	3172		3169	3168	16.882	77.405	CH(99)
4	A'		3155	3152	3148	5.746	115.083	mops1(73),mips1(24)
5	A'	3141		3140	3137	16.812	126.216	mips2(97)
6	A'		3122	3120	3118	21.895	164.248	mips1(74),mops1(25)
7	A'	3106		3108	3104	15.876	70.725	mops2(100)
8	A'		3063	3062	3059	13.095	70.207	mss1(77),mss2(21)
9	A'	3058		3059	3056	11.940	72.444	mss2(78),mss1(20)
10	A'		1670	1669	1667	37.708	16.185	CC(61),bCH(13),bring(10)
11	A'	1657		1654	1653	62.554	16.609	CC(66),bring(10),bCH(8)
12	A'			1562	1559	33.687	10.430	bmopb1(38),bmipb2(19),bmopb2(15),bmipb1(13),CC(5)
13	A'		1545	1542	1540	38.230	8.303	bmipb2(46),bmopb2(35),bmopb1(8)
14	A'			1525	1520	5.543	22.383	bmipb1(71),bmopb1(24)
15	A'	1523		1522	1518	9.631	14.888	bmopb2(60),bmipb1(26),bmopb1(9)
16	A'		1516	1515	1511	9.844	3.020	bmopb1(40),CC(14),bmipb1(13),bCH(8),bmipb2(7),bCOH(5)
17	A'	1476		1475	1472	58.936	2.528	bmipb2(29),bmopb2(21),CC(18),bmopb1(13)
18	A'	1467		1466	1462	2.076	22.472	bmsb2(52),bmsb1(31),CCm(9)
19	A'	1449		1452	1448	0.417	20.656	bmsb1(53),bmsb2(32),CCm(6)
20	A'	1384	1381	1385	1380	51.690	10.706	CO(29),CC(25),CCm(24),bring(17)
21	A'			1362	1358	24.129	2.339	CC(75),bCOH(7)
22	A'	1289		1287	1282	46.021	0.214	bCH(47),CC(20),CCm(9),bCOH(7)
23	A'		1240	1236	1233	38.780	8.112	bCOH(41),CC(25),bCH(23),CCm(7)
24	A'	1217		1213	1209	147.541	1.461	bCH(39),CO(19),CC(15),bCOH(15),CCm(8)
25	A"		1078	1076	1074	0.013	0.801	gCC(35),bmopr2(21),bmopr1(12),bmipb1(11), bmipr1(8)
26	A"	1075		1073	1071	2.177	1.440	gCC(46),bmipr1(16), bmopr2(9),tring(9),bmopr1(6)
27	A'			1071	1070	4.370	1.174	bmipr2(25),bmopr1(18),CCm(13),CC(12),bmipb2(7),bmipr1(6)
28	A'		1065	1069	1066	5.729	1.742	bring(16),bmipr2(14),CC(13),CO(11),CCm(11),CCl(7)
29	A'	1061		1060	1056	46.509	6.272	bring(33),CC(20),CCl(18),bmopr1(9),bmipr2(9)
30	A"			1003	999	0.056	8.183	gCC(29),bring(16),bmipr2(14),CO(10),bmopr1(9),CCm(6)
31	A'		985	982	979	5.258	0.084	CCm(46),CC(16),bring(12),bmipr2(5),bmopr1(5)
32	A"			885	881	14.674	2.308	gCH(75),tring(14),gCO(7)
33	A"	849	848	846	841	17.797	2.798	gCH(76),tring(14),gCO(7)
34	A"			713	709	0.359	0.382	tring(59),gCC(17),gCCl(14),gCO(8)
35	A"	640	644	646	642	27.587	0.632	gCCl(41), bring(38),CO(9),CC(6)
36	A"			607	604	0.071	0.199	gCO(38),tring(33),gCCl(14),gCC(12)
37	A'	592		590	586	0.005	21.987	CCm(36),CC(32),bring(21),CO(6)
38	A'	571	570	569	566	3.716	6.692	bCCl(20),bCCO(20),bCC1(16),bCC2(15),bring(14)
39	A"			531	527	0.667	0.008	gCC(52),tring(41)
40	A'		518	520	517	4.833	1.262	bring(54),bCCO(14),bCC1(10),bCC2(10),CCm(6)
41	A'		396	393	390	0.666	7.486	bring(38),CCl(33),bCC2(8),CC(7),bCC1(7)
42	A"			362	357	117.268	3.423	tOH(91)
43	A"		346	342	337	0.078	0.768	gCCl(53),tring(27),gCC(8)
44	A'			318	313	4.943	0.223	bCCO(48),bCC1(15),bCC2(14),CC(11)
45	A'		295	293	288	2.426	0.440	bCC2(37),bCC1(36),bring(11),CC(6),CCl(5)
46	A'			254	252	0.857	0.512	bCCl(80),bCC1(6),bCC2(6)
47	A"		237	239	235	1.986	3.765	tring(63),gCH(17),gCC(13)
48	A"			194	190	2.196	0.109	gCC(33),tring(21),gCH(18),gCCl(15),gCO(10)
49	A"		158	157	154	1.101	0.153	tm1(58),tm2(22),gCC(10)
50	A"			155	152	0.038	0.112	tm2(62),tm1(23),gCC(6)
51	A"			105	102	0.518	0.025	tring(88)

Abbreviations used: b, bending; g, wagging; t, torsion; s, strong; vs, very strong; w, weak; vw, very weak;

[a] Relative absorption intensities normalized with highest peak absorption

[b] Relative Raman intensities calculated by Eq 1 and normalized to 100.

[c] For the notations used see Table 4.

Table 6. The charge distribution calculated by the Mulliken and Natural Bond Orbital (NBO)

Atoms	Atomic charges	Natural charges (NBO)
C1	0.374185	0.37971
C2	-0.221761	-0.29025
C3	0.185345	-0.00955
C4	-0.205539	-0.06138
C5	0.187264	-0.00975
C6	-0.258643	-0.30125
O7	-0.645969	-0.78303
H8	0.138693	0.25050
C9	-0.528782	-0.65510
Cl10	-0.033790	-0.03103
C11	-0.529334	-0.66205
H12	0.116259	0.24116
H13	0.408484	0.50436
H14	0.168230	0.24168
H15	0.182848	0.24308
H16	0.156554	0.22677
H17	0.169841	0.23326
H18	0.151714	0.23559
H19	0.184400	0.24727

Table 7. The dipole moment (μ) and first-order hyperpolarizibility (β) of 4C35X derived from DFT calculations

β_{xxx}	**-17.398**
β_{xxy}	403.29
β_{xyy}	16.492
β_{yyy}	741.47
β_{zxx}	61.134
β_{xyz}	687.77
β_{zyy}	-14.717
β_{xzz}	-172.96
β_{yzz}	881.28
β_{zzz}	-74.497
β_{total}	34.726
μ_x	0.0215762
μ_y	0.30427845
μ_z	0.18335832
μ	0.7135916

Dipole moment (μ) in Debye, hyperpolarizibility β(-2ω;ω,ω) 10^{-30}esu.

Table 8. Computed absorption wavelength (λ_{ng}) , energy (E_{ng}), oscillator strength (f_n) and its major contribution

n	λ_{ng}	E_{ng}	f_n	Major contribution
1	199.4	6.22	0.0075	H-0->L+0(+51%),H-1->L+1(35%)
2	194.0	6.39	0.0033	H-0->L+1(+42%), H-1->L+0(+42%)
3	167.7	7.39	0.0016	H-0->L+2(+80%)

(Assignment; H=HOMO,L=LUMO,L+1=LUMO+1,etc.)

Conclusions

In the present work, the molecular parameters and frequency assignments for the compound 4C35X were calculated and FT-IR and FT-Raman spectra were recorded. The harmonic frequencies for the title compounds were determined and analyzed at DFT level of theory utilizing B3LYP/6-311+G** basis set. The assignments of most of the fundamentals of the title compound provided in this work are quite comparable. The excellent agreement of the calculated and observed vibrational spectra reveals the advantages of quantum chemical calculations. The various modes of vibrations were unambiguously assigned on the basis of the result of the PED output obtained from normal coordinate analysis. The obtained data and simulations both show the way to the characterization of the molecule and help for spectra studies in the future. The first-order hyperpolarizibility (β_{ijk}) of the novel molecular system of 4C35X is calculated using B3LYP/6-311+G** basis set based on finite field approach. The first-order hyperpolarizability (β_{total}) of 4C35X was calculated and found to be 34.726x10^{-30} esu, which is greater than that of urea (0.1947x10^{-30} esu). The β_{yzz} direction shows biggest value of hyperpolarizability which insists that the delocalization of electron cloud is more on that direction than other directions. Electronic excitation energies, oscillator strength and nature of the respective excited states were calculated by the closed-shell singlet calculation method. The NLO responses can be understood by examining the energetic of frontier molecular orbitals. There is an inverse relationship between hyperpolarizability and HOMO–LUMO.

References

1. Larson, E (1986). "An approach for selection of health care personnel handwashing agents". Infect Control 7: 419–424.

2. M. J. Frisch, G. W. Trucks, H. B. Schlegel, G. E. Scuseria, M. A. Robb, J. R. Cheeseman, G. Scalmani, V. Barone, B. Mennucci, G. A. Petersson, H. Nakatsuji, M. Caricato, X. Li, H. P. Hratchian, A. F. Izmaylov, J. Bloino, G. Zheng, J. L.

Sonnenberg, M. Hada, M. Ehara, K. Toyota, R. Fukuda, J. Hasegawa, M. Ishida, T. Nakajima, Y. Honda, O. Kitao, H. Nakai, T. Vreven, J. A. Montgomery, Jr., J. E. Peralta, F. Ogliaro, M. Bearpark, J. J. Heyd, E. Brothers, K. N. Kudin, V. N. Staroverov, R. Kobayashi, J. Normand, K. Raghavachari, A. Rendell, J. C. Burant, S. S. Iyengar, J. Tomasi, M. Cossi, N. Rega, J. M. Millam, M. Klene, J. E. Knox, J. B. Cross, V. Bakken, C. Adamo, J. Jaramillo, R. Gomperts, R. E. Stratmann, O. Yazyev, A. J. Austin, R. Cammi, C. Pomelli, J. W. Ochterski, R. L. Martin, K. Morokuma, V. G. Zakrzewski, G. A. Voth, P. Salvador, J. J. Dannenberg, S. Dapprich, A. D. Daniels, O. Farkas, J. B. Foresman, J. V. Ortiz, J. Cioslowski, and D. J. Fox, Gaussian, Inc., Wallingford CT, 2009.

3. A.D. Becke, J. Chem. Phys., 98 (1993) 5648.

4. C. Lee, W. Yang, R.G. Parr, Phys. Rev., B37 (1988) 785.

5. A. Frisch, A.B. Nielson, A.J. Holder, Gaussview Users Manual, Gaussian Inc., Pittsburgh, PA, 2000.

6. P. Pulay, G. Fogarasi, G.Pongor, J. E. Boggs, A. Vargha, J. Am. Chem. Soc., 105 (1983) 7037.

7. Yaping Tao, Ligang Han, Yunxia Han and Zhaojun Liu, Spectrochimica Acta Part A: Molecular and Biomolecular Spectroscopy, 137 (2015) 1078-1085.

8. Yu Zhang, Fang Zhang, Kuirong Ma and Guodong Tang, Spectrochimica Acta Part A: Molecular and Biomolecular Spectroscopy, 105 (2013) 352-358.

9. Lijuan Zhang, Dan Yu, Changwu Dong, Min Cheng, Lili Hu, Zhimin Zhou, Yikui Du, Qihe Zhu and Cunhao Zhang, Spectrochimica Acta Part A: Molecular and Biomolecular Spectroscopy, 104 (2013) 235-242.

10. S. Shailajha, U. Rajesh Kannan, S.P. Sheik Abdul Kadhar and E. Isac Paulraj, Spectrochimica Acta Part A: Molecular and Biomolecular Spectroscopy, 133 (2014) 720-729.

11. Sameh Guidara, Habib Feki and Younes Abid, Journal of Molecular Structure, 1080 (2015) 176-187.

12. Katarzyna Piela, Krystyna Holderna-Natkaniec, Mikolaj Baranowski, Tomasz Misiaszek, Jan Baran and M. Magdalena Szostak, Journal of Molecular Structure, 1033 (2013) 91-97.

13. Mohammad Jane Alam and Shabbir Ahmad, Journal of Molecular Structure, 1059 (2014) 239-254.

14. R.S.Mulliken, J.Chem.Phys.23 (1995) 1833-1840.

15. D.A. Kleinman, Phys. Rev. 1962;126,1977.